Dynamic Monte Carlo simulation of spinlattice relaxation of quadrupolar nuclei in solids. Oxygen17 in yttriadoped ceria

Stuart B. Adler, Jacob W. Smith, and Jeffrey A. Reimer

Citation: The Journal of Chemical Physics **98**, 7613 (1993); doi: 10.1063/1.464701
View online: http://dx.doi.org/10.1063/1.464701
View Table of Contents: http://scitation.aip.org/content/aip/journal/jcp/98/9?ver=pdfcov
Published by the AIP Publishing

Dynamic Monte Carlo simulation of spin-lattice relaxation of quadrupolar nuclei in solids. Oxygen-17 in yttria-doped ceria

Stuart B. Adler, Jacob W. Smith, and Jeffrey A. Reimer[a)]
Department of Chemical Engineering, University of California, Berkeley, Berkeley, California 94720-9989

(Received 22 October 1992; accepted 29 January 1993)

Although measurement of spin-lattice relation time (T_1) can provide valuable information about atomic motion in solids, T_1 data for quadrupolar nuclei are often difficult to interpret because the relevant physical interactions cannot be expressed analytically. In order to address this problem, we have developed an extension to the dynamic Monte Carlo method for simulating spin-lattice relaxation of quadrupolar nuclei in solids. In this paper we develop the simulation method generally, and then apply the method to understanding published T_1 measurements of oxygen-17 in yttria-doped ceria. We show that even for simple geometries of motion, multiple time scales for electric field gradient fluctuations are possible, resulting in complex relaxation behavior including multiple T_1 minima. The method can be used to explain and deconvolute data in which these effects are present. In the case of yttria-doped ceria, we show that two experimentally observed T_1 minima result from simultaneous movement of oxygen vacancies and oxygen ions. We discuss the meaning of the kinetic parameters extracted from the data, and show evidence for the relevance of these parameters to bulk vacancy diffusion kinetics.

I. INTRODUCTION

Measurement of nuclear spin-lattice relaxation has been used extensively to study molecular and atomic motion in solids, often with the hope that kinetic parameters extracted from the data are related directly to the mechanistic details of motion. Unfortunately, interpretation of relaxation data is not always straightforward, and extraction of meaningful kinetic parameters can be difficult. This is especially true for quadrupolar nuclei when the dominant mechanism for relaxation is coupling of the nuclear quadrupole to fluctuations of electric field gradients caused by the atomic or molecular motion. Often these fluctuations cannot be expressed analytically even for simple geometries of motion, and thus even if a plausible model for the mechanism of motion is at hand, it may not be obvious how that motion will effect the relaxation measurement. In this paper we address this problem by developing an extension to the dynamic Monte Carlo method for simulating spin-lattice relaxation of quadrupolar nuclei in solids. We then demonstrate the method by reanalyzing published T_1 measurements of oxygen-17 in yttria-doped ceria.

The Monte Carlo method has been used extensively to simulate the thermodynamics of many-bodied systems, and more recently has been extended for obtaining dynamic information as well.[1–4] The dynamic Monte Carlo method relies on the assumption that details of short-time motion in the system, such as vibrations, are unimportant in determining long-time behavior, such as diffusion. Short-time behavior is treated statistically using rules that are consistent with transition state theory and statistical mechanics.[1] The method is especially amenable to systems where restricted geometry results in a finite number of realistic structural conformations, as in crystalline solids or polymers. A simple version of the method has been used previously to simulate spin-lattice relaxation of spin-1/2 nuclei on a cubic lattice.[5] In the first part of this paper we develop an extension to the dynamic Monte Carlo method for calculating spin-lattice relaxation of quadrupolar nuclei in disordered solids. Although we discuss the method in the context of diffusion in a crystalline lattice, the method is quite general and can be modified for other geometries of motion if needed.

In the second part of the paper, we apply the method to analysis of spin-lattice relaxation of oxygen-17 in yttria-doped ceria. Although doped ceria has been well studied, we felt that there were unexplored details in published relaxation data that would be instructive to reinvestigate. The T_1 data for ceria are complex, and the activation energy for oxygen motion extracted from NMR seems to disagree with that determined by other methods. We demonstrate how the dynamic Monte Carlo simulation provides new insights into our understanding the relaxation behavior in this system, and thereby affords a less ambiguous extraction of kinetic parameters from the NMR data.

II. THEORY

A. Quadrupolar relaxation

The spin-lattice relaxation time T_1 is a measurable time constant that describes the rate at which nuclear spin states return to equilibrium following excitation by radio frequency radiation. This return to equilibrium is stochastic, and is caused by fluctuations in the nuclear spin Hamiltonian that occur near the Larmor frequency of the nucleus, ω_0. Since ω_0 is typically 10^7–10^8 Hz, T_1 measurements are sensitive to the MHz frequency motion found in many systems.[6] Typically, the dominant contributor to the spin Hamiltonian for a quadrupolar nucleus in a diamagnetic solid (beside the Zeeman interaction) is the

a)Author to whom correspondence should be addressed.

coupling between the quadrupole moment of the nucleus and the electric field gradient (EFG) at the site of the nucleus. Motion of charges in the lattice relative to the nucleus cause fluctuations in the electric field gradient, resulting in spin-lattice relaxation. For rapid stationary fluctuations in a high magnetic field, the relaxation rate T_1^{-1} is given by the weak collision limit:[7]

$$\left(\frac{1}{T_1}\right)=\frac{9}{160}\frac{(eQ)^2(2I+3)}{\hbar^2 I^2(2I-1)}\left[J_Q^{(1)}(\omega_0)+J_Q^{(2)}(2\omega_0)\right], \tag{1}$$

where (eQ) and I are the quadrupole moment and nuclear spin of the nucleus, and $J_Q^{(1)}(\omega)$ and $J_Q^{(2)}(\omega)$ are the spectral density functions for electric field gradient fluctuations experienced by the nucleus. This expression shows that the relaxation rate is determined by the density of EFG fluctuations at ω_0 and $2\omega_0$.

The EFG at a nucleus may be described by a traceless symmetric tensor with five independent components, which in a spherical basis are described by the lattice functions:

$$V^{(0)}=-2(V_{zz}), \tag{2a}$$

$$V^{(\pm 1)}=\tfrac{2}{3}(V_{xz}\pm iV_{yz}), \tag{2b}$$

$$V^{(\pm 2)}=\tfrac{4}{3}[\tfrac{1}{2}(V_{xx}-V_{yy})\pm iV_{xy}], \tag{2c}$$

where $\{V_{ij}\}$ are the components of the EFG tensor in a Cartesian basis, $\mathbf{V}^{\text{lab}}$, in the reference frame of the magnetic field.[7] The spectral density function $J_Q^{(q)}(\omega)$ is defined to be the Fourier transform of the time autocorrelation function $G_Q^{(q)}(t)$:

$$J_Q^{(q)}(\omega)=2\,\mathrm{Re}\left[\int_0^\infty G_Q^{(q)}(t)e^{-i\omega t}dt\right], \tag{3}$$

where

$$G_Q^{(q)}(t)=\langle V^{(-q)}(t)^* V^{(-q)}(t=0)\rangle \tag{4}$$

describes the time decay of correlation of the electric field gradient experienced by the nucleus. For an ergodic system, the time average in Eq. (4) can be viewed as an ensemble average over all the nuclei in the system.

It is commonly assumed that $G_Q^{(q)}(t)$ is an exponentially decaying function, with time constant τ_c, called the *correlation time*.[6,8–10] If it is also assumed that the fluctuations are the result of an activated process, such as atoms hopping in a crystal, then

$$\tau_c=\tau_c^0\exp\left(+\frac{E_{\text{act}}}{kT}\right), \tag{5}$$

where E_{act} is the activation energy for the fluctuation. These assumptions result in an expression for T_1 that has a minimum where $1/\tau_c\sim\omega_0$, and a slope on an Arrheneous plot [$\ln(T_1^{-1})$ vs $1/T$] equal to $\pm E_{\text{act}}/k$ on either side of the minimum.[8] Fitting of the data allows extraction of the parameters t_c^0 and E_{act} which may be used with an appropriate model to predict macroscopic properties. In general, however, $G_Q^{(q)}(t)$ does not decay exponentially, and in fact is unlikely to do so in systems with complex atomic motion. A nonexponential decay of $G_Q^{(q)}(t)$ means that a single correlation time does not exist, that multiple T_1 minima are possible, and that parameters extracted from the data may be convoluted. The purpose of the dynamic Monte Carlo simulation is to calculate this correlation function explicitly as the simulated system evolves in time.

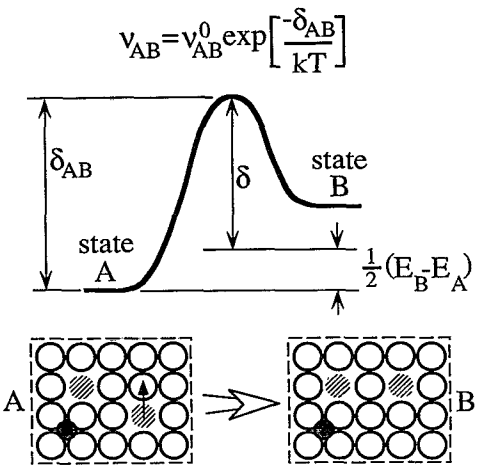

FIG. 1. Schematic of the energetic transition state encountered by a system upon going from one state to another. The dynamic Monte Carlo method uses a rate expression which depends on the height of this transition state, as explained in the text. The example shown at the bottom of the figure is a two-dimensional analog of yttria-doped ceria, in which an oxide ion *vacancy* (hashed circle) exchanges places with an oxide ion (open circle). The energies of the initial and final states are determined by interactions among vacancies and *defects* (small shaded circle).

B. The Monte Carlo method

The dynamic Monte Carlo method involves generating a lattice with a finite number of particles and then allowing this lattice to evolve in time. In yttria-doped ceria the particles we consider are charged atoms on a fluorite crystal lattice, although in general these particles could be atoms, molecules, or parts of molecules in some kind of restricted geometry. For investigations of bulk materials, the lattice normally has periodic boundary conditions.[2] In our case the particles in the system include quadrupolar nuclei which experience fluctuations of electric field gradients produced by other particles. The lattice is allowed to evolve under the set of rules described below, and after the system comes to thermodynamic equilibrium, statistics are accumulated for calculating $G_Q^{(q)}(t)$.

The rules for movement are as follows. For each physically plausible move of the system to another conformation, the system must go through an energetic transition state as shown in Fig. 1. The rate at which this transition may occur is given by

$$\nu_{AB}=\nu_{AB}^0\exp\left(\frac{-\delta_{AB}}{kT}\right), \tag{6}$$

where ν_{AB}^0 is a fundamental, temperature-independent attempt rate for the transition, and δ_{AB} is the energy differ-

ence between the transition state and the initial state, A, of the system. The energy state of the system before and during the transition is determined by energetic interactions between particles in the lattice, as described below for the specific case of yttria-doped ceria. This set of rules ensures consistency with equilibrium statistical mechanics, as well as "proper" dynamics.[4]

There are several ways to implement these rules. We chose to do the following. For each simulation step, the algorithm assesses the transition rates of all the possible moves in the system. The algorithm then executes one of these moves at random according to the relative probability:

$$P_i=\frac{\nu_i}{\sum_{j=1}^{m}\nu_j}, \tag{7}$$

where ν_i is the transition rate of the ith move, and m is the number of possible moves. The amount of time, τ_{step}, consumed during each simulation step is given by

$$\tau_{\text{step}}=\frac{-\ln(P)}{\sum_{j=1}^{m}\nu_j}, \tag{8}$$

where P is a random number between 0 and 1. This method of time accounting preserves the Poisson statistics of the transition events at short times.[3]

During the simulation, statistics are accumulated for calculating $G_Q^{(q)}(t)$ as follows. As the lattice evolves in time, the electric field gradient tensor in the crystal axis system of the lattice, $\mathbf{V}^c$, is calculated at each quadrupolar nucleus by adding the contributions of all sources of electric field gradients in the system. In the case of yttria-doped ceria, field gradients are caused by ionic charges in the fluorite lattice. $\mathbf{V}^{\text{lab}}$ in the axis system of the magnetic field is related to $\mathbf{V}^c$ by rotation about the polar and equatorial angles α and β describing the direction of the magnetic field in the crystal axis system:

$$\mathbf{V}^{\text{lab}}=\mathbf{R}(\alpha,\beta)\mathbf{V}^c\mathbf{R}^{-1}(\alpha,\beta). \tag{9}$$

$G_Q^{(q)}(t)$ is then calculated by taking the ensemble average in Eq. (4) over all the nuclei in the lattice, and over multiple simulations with different random initial conditions. $J_Q^{(q)}(\omega)$, and finally T_1^{-1}, are obtained by fitting $G_Q^{(q)}(t)$ empirically to a sum of exponentials and then taking the analytical Fourier transform. Unfortunately, the disparity in time scales over which $G_Q^{(q)}(t)$ decays often precludes direct numerical Fourier transformation.

So far we have developed a general simulation method for determining the spectral densities of electric field gradient fluctuations experienced by quadrupolar nuclei. We now turn to the specific application of this method to oxygen-17 in yttria-doped ceria.

C. Yttria-doped ceria

Figure 2 shows the fluorite structure of CeO_2. The structure consists of two interpenetrating cubic sublattices, one containing oxygen atoms, the other half-occupied by cerium atoms. Ionic transport in ceria has been shown to occur by migration or diffusion of oxide-ion *vacancies* on the cubic oxygen sublattice.[11,12] These vacancies, which are charged +2 relative to the neutral lattice, are created by reduction of Ce^{4+}, or by doping the parent structure with aliovalent cations, such as Y^{3+}, on Ce^{4+} sites. In yttria-doped ceria, charge neutrality requires that one vacancy is created for every two Y^{3+} *defects*, charged −1 relative to the neutral lattice. At moderate temperatures, most vacancies are trapped by association with immobile defects, which are oppositely charged. As the temperature is increased, vacancies escape to the bulk where they can contribute to transport in the presence of a driving force.

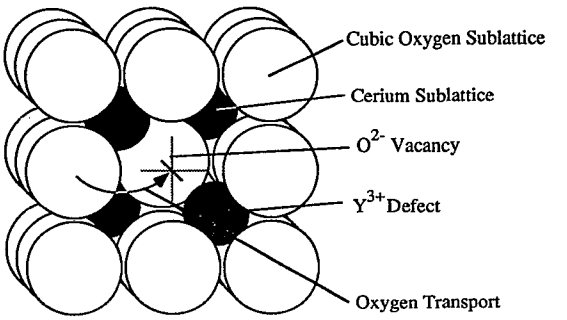

FIG. 2. One unit cell of yttria-doped ceria. Oxygen ions occupy a cubic sublattice, with Ce cations half occupying sites displaced 1/4,1/4,1/4 of a unit cell from oxide ions. The dopant introduces cation *defects* and oxide ion *vacancies* which allow oxygen transport.

As vacancies move, the oxygen nuclei experience electric field gradient fluctuations that result in spin-lattice relaxation. If one assumes that the vacancies move by activated hopping of oxide ions between adjacent sites on the oxygen sublattice, and that this rate is not effected by the presence of the defects, then the average time between hops of a vacancy can be written as

$$\tau_{\text{hop}}=\tau_{\text{hop}}^0\exp\left(+\frac{E_m}{kT}\right), \tag{10}$$

where E_m is the activation energy for vacancy hops in bulk ceria. If one further assumes the existence of a single, activated correlation time τ_c for electric field gradient fluctuations, and the equivalence of Eqs. (5) and (10), then fitting of T_1 data should reveal the preexponential factor τ_{hop}^0 and activation energy E_m for vacancy motion.

Fuda *et al.* have measured the T_1 of ^{17}O in isotopically enriched powdered samples of yttria-doped ceria over a range of temperatures and doping levels.[13,9] Their results for the dilute dopant levels are shown in Fig. 3, along with theoretical fits to the data based on the assumptions implied by Eqs. (5) and (10). The data show a maximum in the relaxation rate at $1000/T=1.8$, which the authors have attributed to EFG fluctuations caused by hopping of oxide ion vacancies. The fits to the data reveal a preexponential factor of 3.6×10^{-13} s and an activation energy of 0.49 eV for site hopping, which are concentration independent at dopant levels below 0.6%. This value for the activation energy is considerably less than 0.65 eV determined from measurements of ionic conductivity and dielectric relaxation.[14,15] In addition to the maximum in T_1^{-1} discussed

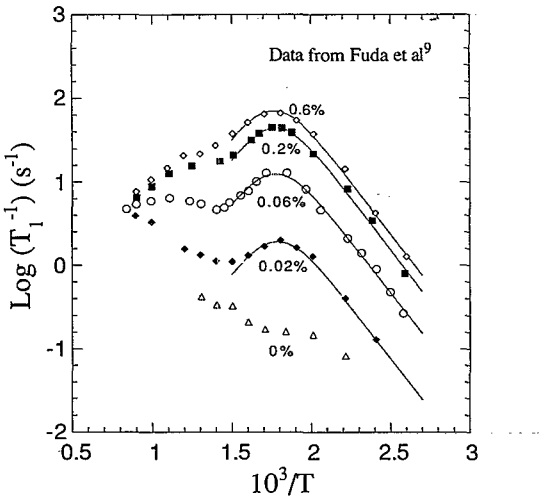

FIG. 3. Measured spin-lattice relaxation rate of yttria-doped ceria as a function of temperature and dopant concentration. Dopant concentrations are quoted in mol % Y_2O_3 in CeO_2. The lines are fits to the data assuming an exponentially decaying electric field gradient correlation function. From Fuda *et al.* (Ref. 13).

above, there is a second, broader relaxation rate maximum at a higher temperature that merges with the first maximum as the dopant concentration increases. At high dopant levels these maxima merge completely.[9] Although the authors could not explain the source of this second T_1 minimum, they did the experiments at different magnetic field strengths to show conclusively that this second relaxation process is a result of motion. Clearly, an analysis which considers a single, activated correlation time is insufficient to fully explain the data.

In order to simulate this system, we set up a fluorite lattice, $11\times11\times11$ unit cells in size, with periodic boundary conditions. Each oxygen site may be occupied by an ^{17}O atom or a vacancy, and defects may occupy cation sites (1/4,1/4,1/4) of a unit cell relative to the oxygen sites. Initially, defects and vacancies are positioned in the lattice at random. The vacancies are then allowed to move by switching places with adjacent ^{17}O atoms according to the rules of the dynamic Monte Carlo method, using the energetics described below. Once the system reaches thermodynamic equilibrium, statistics are acquired for calculating the correlation functions. We consider the system to be at equilibrium when the radial distribution of vacancies around the defects ceases to change with time.

We treat the vacancy–defect interactions using a Coulomb potential in a dielectric medium of pure ceria:

$$\epsilon_{vd}(r)=\frac{q_v q_d}{4\pi\epsilon}\frac{1}{r}, \tag{11}$$

where r is the distance between the vacancy and the defect, q_v and q_d are the charges on a vacancy $(+2)$ and a defect (-1), and ϵ is the permitivity of a dielectric medium of pure ceria, measured by Wang *et al.* to be $25\epsilon_0$.[15] The energy required to separate a vacancy–defect pair to infinity using this potential is 0.492 eV, which is consistent with ionic transport measurements.[16] The vacancy–vacancy interactions were treated similarly using a repulsive potential, $\epsilon_{vv}(r)$, of the same form. The change in the energy of the system upon movement of vacancy (i) is the sum of all changes in the pairwise interactions in the system:

$$(E_B-E_A)_i=\sum_j^d[\epsilon_{vd}(r_{i,j}^B)-\epsilon_{vd}(r_{i,j}^A)] + \sum_{i'\neq i}^{v}{}'[\epsilon_{vv}(r_{i,i'}^B)-\epsilon_{vd}(r_{i,i'}^A)], \tag{12}$$

where the sum includes all particles in the simulated region, as well as "virtual" particles outside the region which exist due to the periodic boundary conditions. For Coulombic forces this is an infinite sum which must be solved using a Fourier series, the method for which is described elsewhere.[16,17] Upon calculating the energy change of the transition, we take the energy of the transition state, δ_{AB}, to be $(1/2)(E_B-E_A)+\delta$, where δ is defined by this expression to be an activation barrier to hopping which may depend on position in the lattice (see Fig. 1). For vacancy moves in the bulk, far from other particles, this barrier corresponds to the hopping activation energy in bulk ceria, E_m. Finally, we assume that ν_{AB}^0 is a spatially invariant constant determined by phonon modes in ceria, and we define it to be $1/t_0$, where t_0 is the average time between hop attempts in a given direction.

Vacancies $(+2)$ and defects (-1) are viewed as point charges for the purpose of calculating the EFG contributions. The electric field gradient at each oxygen nucleus is calculated by summing the contributions from each of the charged particles in the lattice. The contribution of the kth particle to each component of $\mathbf{V}^c$ is given by

$$(V_{ij}^c)_k=\frac{(1-\gamma^\infty)}{4\pi\epsilon}\left[\frac{\partial^2\left(\frac{1}{r}\right)}{\partial i\partial j}\right]_{\mathbf{r}_k}, \tag{13}$$

where $\mathbf{r}_k$ is the relative coordinate between the nucleus and the kth particle and γ^∞ is the Sternheimer antishielding factor for O^{2-}, assumed to be a constant.[8,18] Since the contributions to $G_Q^{(q)}(t)$ scale as $(1/r^3)^2$, it is appropriate to terminate this sum at a distance of about five nearest neighbors.

Note that in general $G_Q^{(q)}(t)$, and therefore T_1^{-1}, depend on the orientation of the lattice with respect to the magnetic field. However, in the case of a powdered sample of yttria-doped ceria, consideration of oxygen self-diffusion rates shows that during the time scale of the NMR experiment, ^{17}O atoms are likely to self-diffuse among multiple crystallites with different orientations. We will assume this to be the case, and that this results in a single, average

relaxation rate for the entire sample, as has been observed experimentally.[13] The proper way to obtain this average is to extend the ergodicity of the system to reflect the time average over crystallite orientations α and β. One method would be to combine the results of many simulations with a spherical distribution of crystallite orientations. We choose the less computer-intensive method of simplifying Eq. (4) by averaging over α and β analytically. This requires reexpressing the lattice functions $V^{(q)}$ in terms of the crystal axis system, as a function of α and β, and then integrating over a spherical distribution. After some algebra the result is

$$G_Q^{(1)}(t)=\frac{4}{135}\left\langle\left\langle \begin{array}{c} 2[V_{xx}^c(t)V_{xx}^c(0)+V_{yy}^c(t)V_{yy}^c(0)+V_{zz}^c(t)V_{zz}^c(0)] \\ +6[V_{xz}^c(t)V_{xz}^c(0)+V_{yz}^c(t)V_{yz}^c(0)+V_{xy}^c(t)V_{xy}^c(0)] \\ +V_{xx}^c(t)V_{zz}^c(0)+V_{zz}^c(t)V_{xx}^c(0) \\ +V_{yy}^c(t)V_{zz}^c(0)+V_{zz}^c(t)V_{yy}^c(0) \\ +V_{xx}^c(t)V_{yy}^c(0)+V_{yy}^c(t)V_{xx}^c(0) \end{array} \right\rangle\right\rangle', \tag{14}$$

and $G_Q^{(2)}(t)=4G_Q^{(1)}(t)$, where $\{V_{ij}^c\}$ are the components of $\mathbf{V}^c$ in the lattice coordinate system, and the prime on the average indicates the reduced ensemble. This expression is equivalent to Eq. (4). Such a procedure is useful in the case where the local orientation of the simulated region is only representative of a subset of the ensemble.

For convenience, the simulation is actually implemented using a dimensionless form of the equations presented here, producing a dimensionless $^*G_Q^{(q)}(t)$ and $^*T_1^{-1}$, related to the dimensional quantities by

$$G_Q^{(q)}(t)=\frac{e^2}{(4\pi\epsilon_0)^2a^6}\,{}^*G_Q^{(q)}(t) \tag{15a}$$

and

$$\left(\frac{1}{T_1}\right)=\frac{9}{160}\frac{(eQ)^2(2I+3)}{\hbar^2I^2(2I-1)}\frac{(1-\gamma^\infty)^2e^2t_0}{(4\pi\epsilon)^2a^6}\left(\frac{1}{{}^*T_1}\right), \tag{15b}$$

where a is the vacancy hop distance (half the cubic lattice parameter), e is the unit charge, and t_0 is the preexponential factor for move attempts, as defined previously. Reporting the results in dimensionless form is adequate for investigating the temperature dependence of $\ln(T_1^{-1})$, although a note will be made at the end of the results regarding the consistency of the scaling factor in Eq. (15b) with the data.

III. RESULTS AND DISCUSSION

Before presenting final simulation results for $^*T_1^{-1}$, it is instructive to look first at the results of simulations in which we allow the vacancies to undergo a random walk through the lattice. We achieve a random walk by excluding from the simulation Coulombic interactions between charged particles in the lattice; i.e., $\epsilon_{vd}(r)=\epsilon_{vv}(r)=0$. We set the barrier to vacancy hopping, δ, to be 0.49 eV everywhere following the analysis of Fuda *et al.*[13] Figure 4 shows the results for $^*T_1^{-1}$ as a function of temperature and dopant concentration. The results agree qualitatively with the experimental observations. The relaxation rate increases with dopant concentration, and there are two T_1^{-1} maxima. Furthermore, the higher temperature maximum merges with the low temperature maximum as the dopant level is increased. The main deviation of these simulation results from the data is that the high temperature T_1^{-1} maximum occurs at a much lower temperature experimentally than the simulations predict, and is spread over a wider range of temperatures (see Fig. 3).

These two T_1^{-1} maxima can be understood by realizing that a single motional process, the motion of vacancies, results in multiple time scales for electric field gradient fluctuations. Oxygen nuclei experience fluctuations due to motion of nearby charged vacancies, which must occur on the time scale of a few vacancy hops. There is a second process, however; oxygen nuclei also experience fluctuations as a result of their own motion relative to stationary charged defects in the lattice. Since individual oxygen nuclei move by infrequent collisions with vacancies, the second process occurs on a much slower time scale and with a rate that depends on the vacancy concentration. For a

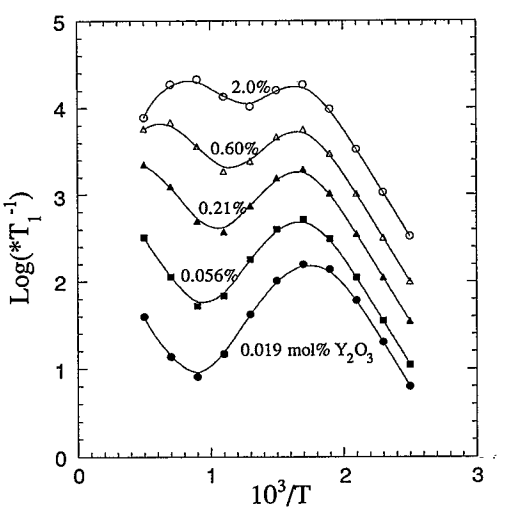

FIG. 4. Simulated spin-lattice relaxation for the case of a random walk (no particle–particle interactions), as a function of temperature and dopant concentration (mol % Y_2O_3). The relaxation rate is nondimensional as explained in the text. The lines which connect the points are to aid the eye, and do not represent theoretical fits.

random walk, the frequency at which a specific oxygen hops, ν^{oxy}, will be related to the vacancy hopping frequency, ν^{vac}, by the ratio of the vacancy-to-oxygen concentrations:

$$\frac{\nu_{vac}}{\nu_{oxy}}=\frac{c_{oxy}}{c_{vac}}. \tag{16}$$

For the dopant levels we consider here, the vacancy concentration is small ($<1\%$), so that the separation in these time scales can be quite large. Fluctuations associated with these two time scales reach the Larmor frequency of the nucleus at substantially different temperatures, producing two T_1 minima, one of which has a position which is concentration dependent.

Previous workers have shown experimentally that multiple species undergoing motion with different correlation times can result in more than one T_1 minimum.[10,19] It has also been shown theoretically that diffusion of vacancies in crystals may produce fluctuations of both the dipolar and quadrupolar interactions, resulting in two different correlation times.[7] However, we see here that even with a single motional process (the hopping of vacancies), and a single relaxation mechanism (quadrupolar), there may be multiple T_1 minima. As with these previous studies, it is tempting to divide $G_Q^{(q)}(t)$ into two separate correlation functions, with separate but related correlation times [e.g., related by Eq. (16) for a random walk]. In general, however, this approach is problematic because there is really only one relaxation mechanism and one process of motion, and so it is ambiguous as to where such a division might be made. Rather, it is more appropriate to consider $G_Q^{(q)}(t)$ to be a nonexponential function to which the concept of a correlation time does not really apply.

The complex nonexponential behavior of $G_Q^{(q)}(t)$ can be seen in the results of simulations which include Coulombic interactions between charged particles. Figure 5 shows a typical decay of $^*G_Q^{(q)}(t)$, under the conditions explained in the figure. The time axis is nondimensional so that each unit of time corresponds to the average time interval between hops of an individual vacancy. Figure 5 shows clearly that $G_Q^{(q)}(t)$ decays nonexponentially with two primary time scales, as implied by Eq. (16) for a random walk. However, Eq. (16) is only qualitatively correct. For a dopant concentration of 0.056%, the ratio of c_{oxy} to c_{vac} is ~ 3000, much larger than the ratio of primary time scales (~ 170) seen for $G_Q^{(q)}(t)$ in Fig. 5. Thus oxygen nuclei appear to move much more frequently than predicted for a random walk. Moreover, the two time scales in Fig. 5 cannot be assigned unambiguously; in fact, we generally need four or five exponentials to accurately parametrize $^*G_Q^{(q)}(t)$ for further analysis.

These effects can be understood by noting that since the magnitude of the electric field gradient around a charge depends on $1/r^3$, oxygen nuclei near defects are primary contributors to the ensemble average in $G_Q^{(q)}(t)$. These oxygen nuclei tend to hop more frequently than oxygen in the bulk because the defects attract a high local concentration of mobile vacancies. The radial distribution of vacancy concentration around the defects also tends to spread out

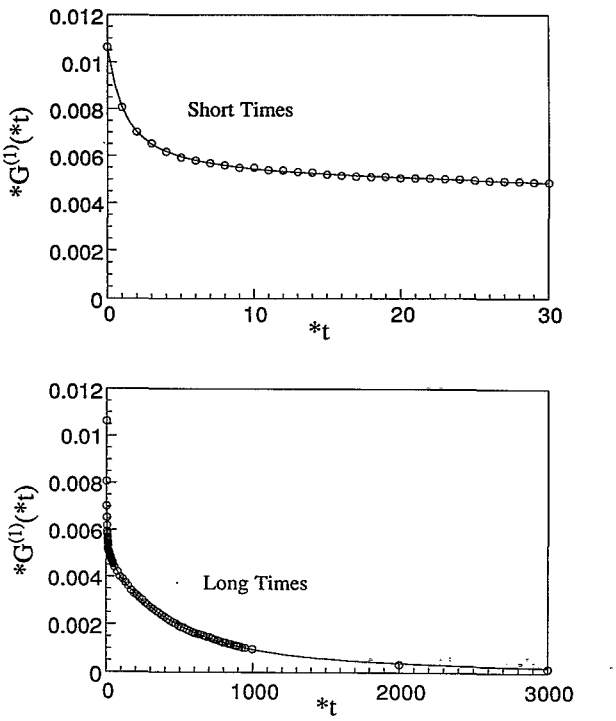

FIG. 5. Simulation results for the decay of the electric field gradient correlation function $^*G_Q^{(q)}(^*t)$. The two graphs share a common y axis, but the time axes differ in scale by a factor of 100. Both axes are nondimensional so that each unit of time corresponds to the average time interval between hops of an individual vacancy. The line is an analytical fit of the data to five decaying exponentials (Ref. 24). The dopant concentration is ~ 0.056 mol %, $\delta=0.49$ eV, and $t_0=3.6\times10^{-13}$ s everywhere, and $T=1000$ K. This simulation represents an ensemble average over $\sim 10^4$ ^{17}O nuclei, and 250 runs with different random defect configurations, requiring ~ 60 CPU min on a Cray XM-P/28.

the time scale for oxygen motion. Observation of the actual vacancy trajectories shows that clustering of vacancies around defects persists even above 1000 K, where the high temperature maximum in T_1^{-1} occurs. To a lesser extent this blending of the two time scales is also a result of the fact that $G_Q^{(q)}(t)$ is not truly exponential for diffusive processes.[20] However, the dominant effect is the Coulombic attraction, which merges the two time scales appreciably.

This merger of the time scales helps to explain the poor agreement between the data and simulations which only consider a random walk (Fig. 4). Figure 6 shows results for simulations of $^*T_1^{-1}$ in which we include the effect of the Coulombic interactions on the system. These results are for a dopant concentration of 0.056 mol %, as a function of temperature. For case A, we set $t_0=3.6\times10^{-13}$ s and $\delta=0.49$ eV everywhere, following Fuda's analysis. Case B (discussed later) is similar, but has $\delta=0.70$ eV for hops between sites adjacent to a defect. Case C is experimental data from Fig. 3 for a 0.06% dopant concentration, rescaled for comparison. In case A we see that including the particle interactions causes the two T_1^{-1} maxima to be broader and much closer in temperature than for a random walk. This result is consistent with our observations about the decay of $^*G_Q^{(q)}(t)$ shown in Fig. 5, where the time scales of vacancy and oxygen motion are much closer than

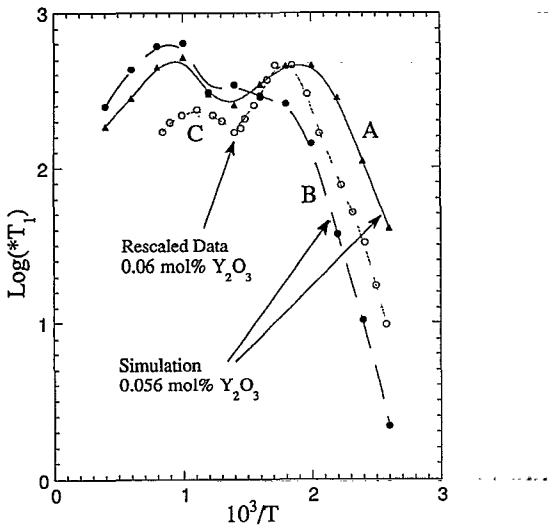

FIG. 6. Simulated spin-lattice relaxation for the case of Coulombic interactions among charged vacancies and defects. Case *A*: $\delta=0.49$ eV everywhere; case *B*: $\delta=0.49$ eV everywhere except for jumps between sites adjacent to a defect, where $\delta=0.70$ eV. Case *C* is the measured relaxation rate for 0.06 mol % yttria/ceria (Ref. 13), rescaled from Fig. 3 so that the rate at the low temperature T_1^{-1} maximum matches the nondimensional simulation. The lines are to aid the eye, and do not represent theoretical fits.

predicted by Eq. (16) and are not clearly separable. Although the agreement between the simulation and the data is not quantitative, we believe that the simulation is successful in reproducing the basic physics in this system.

We now examine the effect of the nonexponential behavior of $G_Q^{(q)}(t)$ on the meaning of kinetic parameters extracted from the data. Based on the analysis so far, we know that the low temperature T_1^{-1} maximum is associated with the time scale for vacancy motion, as assumed by Fuda *et al.* in their analysis.[13] Careful examination of Fig. 6, case *A* shows that the kinetic parameters extracted from the low temperature $*T_1^{-1}$ maximum are in fact indicative of bulk vacancy motion. The slope at low temperatures is ~ 0.45 eV, corresponding closely to the actual barrier height of $\delta=0.49$ eV. In addition, the preexponential factor extracted from the position of the $*T_1^{-1}$ maximum using Eq. (5) is $\sim 2\times 10^{-13}$ s, quite close to $t_0=3.6\times 10^{-13}$ s used in this simulation. This insensitivity of the parameters to the presence of the dopant supports the argument originally presented by Fuda *et al.* that from the perspective of an ^{17}O nucleus there is little distinction between vacancies hopping "productively" in the bulk or "unproductively" when trapped around a defect at low temperature.[13] This distinction only becomes important for bulk transport.[13,16,21]

This analysis makes the assumption that in the real system barriers to hopping around the defects are the same as in the bulk. However, calculations using the method of lattice statics show that this may be a poor assumption.[21] These calculations predict the same bulk activation energy extracted from the NMR data, $E_m=0.49$ eV, but they show that the barriers between sites adjacent to a defect are 0.21 eV higher than in the bulk. To test the hypothesis of uniform barrier heights, we performed simulations which included this extra barrier of 0.21 eV, with the results shown in Fig. 6, case *B*. The results are heavily skewed, almost to the point of eliminating the low temperature T_1^{-1} maximum. The slope at low temperatures is ~ 0.7 eV, corresponding to the higher barrier. Comparison with data shows poor qualitative agreement, suggesting that the barriers are uniform in the real system. We surmise that at the high temperatures under consideration, strong vibrational fluctuations in the lattice structure are active, tending to equalize the hopping barriers. The method of lattice statics, which does not consider kinetic effects, is unable to take lattice vibrations into account. An interesting test of these ideas would be to try to calculate the dynamic transition state energies more rigorously using molecular dynamics or importance-sampling methods.[1]

Leveling of the potential surface as a result of active phonons may explain the difference between the bulk migration energy determined by NMR, $E_m=\sim 0.5$ eV, and the value determined by measurements of dielectric relaxation, $E_m=\sim 0.65$ eV.[14] In the dielectric experiment, electric dipoles caused by vacancy–defect pairs are polarized in an electric field at sub-0 °C temperatures and then allowed to relax to equilibrium as the temperature is raised to ambient. A current is measured as a function of temperature and the activation energy for the trapped vacancies to hop around their defect associates is extracted from the results. As with NMR data, the analysis assumes that the measured hopping barrier is the same as in the bulk. Phonon modes, however, which appear to equalize the barriers at high temperature may be quenched at −70 °C where the dielectric relaxation measurement is made. If at low temperature the barriers are higher near defects than in the bulk as the static lattice calculations suggest, then the dielectric measurement, which is sensitive primarily to these higher barriers, yields a higher value for the activation energy than the actual bulk migration energy. Evidence for these higher barriers can be found by careful examination of the NMR data shown in Fig. 3. At all dopant levels the slope increases slightly near the lowest temperatures of measurement, suggesting that as the temperature decreases, the barriers for vacancy hops near defects become higher. We believe that the NMR experiment, which is performed at more relevant temperatures than the dielectric experiment, may provide a better measure of the bulk migration energy, with $E_m=\sim 0.5$ eV. This value is consistent with measurements of ionic conductivity in ceria at low dopant concentrations.[16]

Finally, we make a comment about the consistency of the scaling factor between T_1^{-1} and $*T_1^{-1}$ calculated from Eq. (15b) with that taken from the data. This comparison is difficult because there is a great deal of uncertainty in the value of the Sternheimer factor, which tends to depend strongly on the coordination of the atom. If we take γ^∞ to be an adjustable parameter, and then scale the low temperature $*T_1^{-1}$ maximum in Fig. 6, case *A* to the measured T_1^{-1} value of $\sim 14\ s^{-1}$ at 0.06% yttria, we extract a value of $\gamma^\infty=-185$. This value is well within the range reported

in the literature for closed shell $^{17}O^{2-}$ ions, calculated using Hartree–Fock methods to be between -28 and -950.[22] This range represents a change from a highly "contracted" ion in Mg ^{17}O to a free ion in a vacuum.[22,23]

IV. CONCLUSIONS

We conclude that the dynamic Monte Carlo method is a useful technique for simulating complex spin-lattice relaxation behavior of quadrupolar nuclei in solids. We find that even in the simple case of a random walk on a cubic lattice, there may be multiple time scales of electric field gradient fluctuations, which are further convoluted by energetic interactions in the lattice. This causes a breakdown in the assumption that $G_Q^{(q)}(t)$ decays exponentially, and allows the presence of multiple T_1 minima. Careful analysis may be needed to ensure that kinetic parameters extracted from T_1 measurements of quadrupolar nuclei, such as ^{17}O, are meaningful. We believe that the methods presented in this paper are a useful tool for aiding in this type of analysis.

In the case of yttria-doped ceria, the simulations show that at low dopant concentration, the kinetic parameters extracted from the low-temperature T_1^{-1} maximum are related meaningfully to vacancy hopping events, even in the presence of Coulombic particle interactions. We also find that nonuniformity of the hopping barriers due to the presence of the defects is inconsistent with observed data. This insensitivity of the measurement to the presence of the dopant is quite significant, because it implies that parameters extracted from NMR on lightly doped samples are indicative of bulk kinetics, with $E_m \sim 0.5$ eV and $t_0 \sim 3.6 \times 10^{-13}$ s, as reported by Fuda *et al.*[13] We have found this result to be quite useful in the analysis of the macroscopic transport properties of yttria-doped ceria, as discussed elsewhere.[16]

ACKNOWLEDGMENTS

The authors wish to acknowledge members of the molecular modeling group in the department of Chemical Engineering for many helpful discussions. The authors also wish to acknowledge the assistance of the Visualization Lab in the College of Chemistry under National Institutes of Health Grant No. 850RR05651A. J.A.R. is a Henry and Camille Dreyfus Teacher–Scholar Fellow.

[1] A. F. Voter and J. D. Doll, J. Chem. Phys. **82**, 80 (1985).
[2] K. Mansfield and D. N. Theodorou, Macromolecules **22**, 3143 (1989).
[3] R. L. June, A. T. Bell, and D. N. Theodorou, J. Phys. Chem. **95**, 8866 (1991).
[4] H. C. Kang and W. H. Weinberg, J. Chem. Phys. **90**, 2824 (1989).
[5] D. A. Faux, D. K. Ross, and C. A. Sholl, J. Phys. C **19**, 4115 (1986).
[6] A. V. Chadwick, J. Chem. Soc. Faraday Trans. **86**, 1157 (1990).
[7] D. Wolf, *Spin-Temperature and Nuclear-Spin Relaxation in Matter, Basic Principles and Applications* (Clarendon, Oxford, 1979).
[8] C. P. Slichter, *Principles of Magnetic Resonance*, 3rd ed., Vol. 1 in Springer Series in Solid-State Sciences (Springer-Verlag, Berlin, 1989).
[9] K. Fuda *et al.*, J. Phys. Chem. Solids **46**, 1141 (1985).
[10] A. F. Alders *et al.*, Solid State Ion. **9&10**, 539 (1983).
[11] P. Kofstad, *Nonstoichiometry, Diffusion, and Electrical Conductivity in Binary Metal Oxides* (Krieger, Malibar, FL, 1983).
[12] B. C. H. Steele, in *High Conductivity Solid Ion Conductors*, edited by T. Takahashi (World Scientific, Singapore, 1989).
[13] K. Fuda *et al.*, J. Phys. Chem. Solids **45**, 1253 (1984).
[14] D. Y. Wang and A. S. Nowick, J. Chem. Phys. Solids **44**, 639 (1983).
[15] D. Y. Wang *et al.*, Solid State Ion. **2**, 95 (1981).
[16] S. B. Adler and J. W. Smith (submitted).
[17] A more complete description of this technique is discussed by D. M. Heyes, J. Chem. Phys. **74**, 1924 (1981).
[18] A. Abragam, *Principles of Nuclear Magnetism* (Clarendon, Oxford, 1961).
[19] B. Gunther and O. Kanert, Acta Metall. **31**, 909 (1983).
[20] R. Kimmich and G. Voight, Z. Naturforsch **33a**, 1294 (1978).
[21] A. D. Murray, G. E. Murch, and C. R. A. Catlow, Solid State Ion. **18&19**, 196 (1986).
[22] E. A. C. Lucken, *Nuclear Quadrupole Coupling Constants* (Academic, New York, 1969).
[23] G. Burns and E. G. Wikner, Phys. Rev. **121**, 155 (1961).
[24] The exponential fitting of $G^{(q)}(t)$ was accomplished using software provided by Berkeley Scientific Associates, P.O. Box 5308, Berkeley, CA 94705-0308.